ANALYSIS OF ELECTROSTATIC ION-CYCLOTRON INSTABILITY DRIVEN BY PARALLEL FLOW VELOCITY SHEAR

R.K. Tyagi*, K.K. Srivastava*, R.S. Pandey**

**Department of Mechanical Engineering,*
Birla Institute of Technology Mesra Ranchi, Jharkhand, India, tyagi_rk1@rediffmail.com
***Department of Applied Physics,*
Amity School of Engineering and Technology, Amity University Utter Pradesh, Noida, India

Introduction

In the recent past considerable attention has been given to the study of dynamics that governs the release of free energy associated with sheared flows in magnetohydrodynamics (MHD) and in plasma physics. Sheared flows are the dominant features found in space plasma. Simulation of ion-cyclotron mode in a magneto-plasma with transverse inhomogeneous electric field for a Maxwellian plasma suggested that electrostatic waves with the frequencies of the order of ion-cyclotron frequencies could be destabilized as a result of coupling of regions of positive and negative ion energy of waves [1–3]. A rigorous analytical treatment using MHD approach has established the existence of two modes (i) large wavelength Kelvin-Helmholtz (K-H) mode and (ii) shear wavelength ion-cyclotron mode.

In fusion plasma a sheared flow has been found to modify significantly the magneto-hydrodynamic equilibrium and ballooning stability of toroidal confinement devices [4, 5]. More importantly, shear driven turbulence can have a significant effect on particle, momentum and energy transport. Velocity shear has been recently identified as an important element in the transition from low confinement (L) to high confinement (H) mode in tokomak plasmas [6–9].

Parallel velocity shear (PVS) is a plasma configuration with ion flow parallel to the magnetic field, but with a velocity gradient transverse to B. PVS is commonly observed along the Earth’s auroral field lines and in association with magnetic field-aligned current may excites ion cyclotron instability. Ganguli et al. [10], using Ganguli et al. [1, 2] and Nishikawa et al. [3], Vlasov theory and particle-in-cell (PIC) simulation, have analyzed the effect of inhomogeneous parallel ion flow on the excitation of electrostatic ion cyclotron (EIC) waves in an attempt to understand in-situ observations of these waves in the presence of levels of field-aligned currents that were generally subcritical waveforms. They discovered that ion flow gradients could give rise to a new class of ion-cyclotron waves driven by “inverse cyclotron damping” even in the absence of field-aligned current.

Furthermore the ion flow gradient mechanism can drive the multiple cyclotron harmonics giving rise to “spiky” waveforms has been observed on FAST S/C [11]. Using an extension of the early work of D’Angelo [12] on shear driven (K-H) waves, Merlino [13] used a purely fluid treatment that also included a density gradient to show that the parallel velocity shear could excite EIC waves in plasma with no current.

In the result of a series of experiments, investigating the effect of a parallel velocity shear on ion-cyclotron waves, it has been demonstrated that PVS can be an important excitation mechanism of this plasma mode. It is important to note that in a Q-machine, EIC wave growth without shear has been observed in current free plasma when free energy due to parallel velocity shear was available. PVS is capable of generating a multiple EIC spectrum with high order harmonics having multitudes comparable to the fundamental. Electrostatic ion-cyclotron instability lead by magnetic field-aligned current was first observed in a narrows current channel (width < ion gyro-radius) in a Q-machine [14]. Many of the characteristics of this instability that have been investigated experimentally were in agreement with the local theory of Drummond and Rosenbluth [15] appropriate to a uniform magnetized plasma, in which electron drift along B field lines with the same drift velocity at all points in plasma [16, 17]. The effect of a transverse gradient in the plasma flow velocity parallel to the magnetic field on the excitation of EIC waves has also been analyzed by Ganguli et al. [10]. They showed that ion flow gradients (parallel velocity shear) can give rise to a new class of ion cyclotron waves via inverse cyclotron damping, with a resulting spectrum of multiple cyclotron harmonics. The effect of parallel velocity shear on EIC wave excitation was studied experimentally by Agrimson et al. [18], who pointed out that the typical configuration used to study EIC wave production in the laboratory necessarily included the presence of parallel ion flow with transverse shear. These

© Tyagi R.K., Srivastava K.K., Pandey R.S., Электронная обработка материалов, 2011, 47 (4), 150–159.

experiments provided clear evidence that parallel velocity shear does play a role in the excitation of EIC waves. Further observations of inverse ion-cyclotron damping induced by PVS have also been published by Teodorescu et al. [19].

Experimental results indicate that the presence of parallel velocity shear may lead to the excitation of the instability, even in narrow current filaments that would otherwise not sustain the instability [20]. The instabilities associated with velocity shear transitions separating plasmas moving in opposite directions have been considered [21]. From one semi-infinite plasma streaming with velocity v<0 the transition can be of the so called ion dominated (ID) type where the confining current is only due to the ions and the typical width of the transition is of the order of a typical ion Larmor's radius. In this kind of transition the electrons are electrostatically confined. For $v>0$ the transition can be of the so called electron dominated (ED) type where the confining current is only due to electrons while the ions are electrostatically confined. The ED transition has a typical width of the order of a mean electron Larmor's radius. It has been shown [22] that these two kinds of transition correspond to the two boundaries of a streaming finite plasma beam, one of the boundaries being of the ED type white the other boundary is of the ID type.

There has been considerable interest in recent years in studying the possibility of destabilizing space plasmas with velocity shears. There have, in particular been both direct and indirect evidence for sharp horizontal structures in field-aligned currents [23–26]. The two phenomena, intense bursts of field-aligned currents and large localized ion up flows have been shown to be on the edge of auroral arcs, where narrow but intense parallel current densities also exist.

Interest has also been created in the role played by horizontal shears in field-aligned flows in the excitation of plasma waves in ionospheric and magnetospheric plasmas. Earlier theoretical study suggested and using of the fluid theory that in the presence of collisions, the horizontal shears in the field-aligned ion velocity could produce very low frequency modes in the frame of reference of moving F-region plasma at an angle very close to perpendicular to the magnetic field. Gavrishchaka et al. [27] concluded that the current driven electrostatic ion-cyclotron mode could be excited with parallel drifts significantly below the critical drift for homogenous EIC and also that infinitesimal shears could destabilize waves. Gavrishchaka et al. [28] explored the weak and strong shear limits of the earlier paper to conclude that for weak shears the minimum field-aligned currents were included much smaller than the critical currents for EIC instabilities. Within the fluid limit (requiring in particular that $T_e>>T_i$), it was found that collisions and Larmor's radius corrections both acted to modify the threshold conditions in the regimes explored by Basu and Coppi [29] and Gavrishchaka et al. [27]. In particular, collisions usually meant that the plasma could no longer become unstable to infinitesimal shears, however, shears always introduced a new zero current mode for $\omega/k\alpha_s < 1$ (where α_s be the thermal velocity) for moderate shears.

In the case of parallel flow shear experiments performed in the Q-upgrade machine it is found that ion-cyclotron instability is originally excited by applying positive bias potentials to a small disc electrode adjusted at the centre of a magnetized plasma column. This instability is enhanced by shear and is suppressed by the larger shear. In the case of perpendicular flow shear experiments on the other hand the ion cyclotron instability is excited by the small disc electrode and suppressed by only the slight shear. The perpendicular shear is found to suppress both the current driven type and the potential driven type instabilities which can be excited by changing the bias voltage applied to the small disc electrode.

Three dimensional electrostatic particle simulations recently performed in order to investigate the effects of ion flow velocity shear, in detail have shown that the parallel velocity shear of the ion flow can excites these low frequency instabilities and the excited instabilities are localized at the velocity shear region. Parallel velocity shear is a plasma configuration with ion flow parallel to the magnetic field, but with a velocity gradient transverse to B. It is commonly observed along the Earth's auroral field lines and in association with magnetic field-aligned currents, may excite ion-cyclotron waves. In the present paper the effect of PVS on the excitation of electrostatic ion-cyclotron waves in plasma has been studied with and without field-aligned currents in laboratory conditions.

Analysis

Spatially homogeneous anisotropic plasma subjected to an external magnetic field $\mathbf{B_0} = \mathbf{B_0}\hat{\mathbf{e}}_\mathbf{z}$ and an inhomogeneous DC electric field $\mathbf{E_0(x)} = \mathbf{E_0(x)}\hat{\mathbf{e}}_\mathbf{x}$ has been considered. In order to obtain the dispersion relation, the Vlasov-Maxwell equations are linearized for inhomogeneous plasma by small perturbations of E_1, B_1 and f_{s1}. These are perturbed quantities and are assumed to have harmonic dependence as exp $i(\mathbf{kr}-\omega t)$.

The linearized Vlasov equations obtained by separating the equilibrium and non equilibrium parts following the technique of Misra and Pandey [30] and Pandey et al. [31] in units of $c=1$ (c is the speed of light) are given as:

$$v\frac{\partial f_{s0}}{\partial r}+\frac{e_s}{m_s}\left[E_0(x)+(v\times B_0)\right]\left(\frac{\partial f_{s0}}{\partial v}\right)=0\ , \tag{1}$$

$$\frac{\partial f_{s1}}{\partial t}+v\frac{\partial f_{s1}}{\partial r}+\left(\frac{F}{m_s}\right)\left(\frac{\partial f_{s1}}{\partial v}\right)=S(r,v,t)\ , \tag{2}$$

where the force is defined as $F = mdv/dt$.

$$F=e_s\left[E_0(x)+\left(v\times B_0\right)\right]\ . \tag{3}$$

The particle trajectories are obtained by solving the equation of motion defined from equation (3) and $S(r, v, t)$ is defined as:

$$S(r,v,t)=\left(-\frac{e_s}{m_s}\right)\left[E_1+v\times B_1\right]\left(\frac{\partial f_{s0}}{\partial v}\right)\ . \tag{4}$$

The method of characteristics solution is used to determine the perturbed distribution function f_{s1}. This is obtained from equation (2) by

$$f_{s1}(r,v,t)=\int_0^{\infty}S\left\{r_0\left(r,v,t^{`}\right),v_0\left(r,v,t^{`}\right),t-t^{`}\right\}dt'\ , \tag{5}$$

where the index s denotes species.

We transformed the phase space co-ordinate system from $(r,\ v,\ t)$ to $(r_0,\ v_0,\ t\text{-}t^{`})$. The particle trajectories obtained by solving equation (3) for the given external field configuration by Misra and Tiwari [32] are given as:

$$x(t)=x_0+\frac{v_\perp}{\Omega_s}\left(1+\frac{\overline{E}'(x)}{4\Omega_s^2}\right)\left[\sin\left(\theta-\Omega_s t\right)-\sin\theta\right], \tag{6}$$

$$y(t)=y_0+\Delta+\frac{v_\perp}{\Omega_s}\left(1+\frac{3}{4}\frac{\overline{E}'(x)}{4\Omega_s^2}\right)\left[\sin\left(\theta-\Omega_s t\right)-\cos\theta\right],$$

$$z(t)=z_0+v_{||}t\ .$$

Here, θ is the angle between the vectors **k** and $\mathbf{B_0}$. The values $E^{'}(x),\ E^{''}(x)$ are the derivatives of $E(x)=E_{0x}\left(1-\frac{x^2}{a^2}\right)$. Herewith:

$$\Delta=\frac{\overline{E}(x)\ t}{\Omega_s}\left[1+\frac{E''(x)}{E(x)}\cdot\frac{1}{4}\left(\frac{v_\perp}{\Omega_s}\right)^2..............\right],\ \overline{E}(x)=\frac{e_sE(x)}{m_s}\ ,\ \Omega_s=\frac{e_sB_0}{m_s}\ .$$

It should be noted that $\Delta'=\frac{\partial\Delta}{\partial t}$ represents the drift velocity. The value a is the scale length of electric field inhomogeneity. It is thought to be comparable to the mean ion gyro-radius, but larger than the Debye's length. When $x^2/a^2 < 1$, $E(x)$ becomes a constant uniform field.

After some lengthy algebraic simplifications following techniques out lined in Misra and Pandey [30] the time integration gives the perturbed distribution function as:

$$f_{s1}(r,v,t)=\frac{ie_s}{m_s\omega}\sum_{m,n,p,g}J_n(\lambda_1)J_m(\lambda_1)J_p(\lambda_2)J_g(\lambda_2)e^{i(m-n)(\pi/2+\theta)}e^{i(g-p)(\pi/2+\theta)}\times$$

$$\times\left[E_{1x}U^*+V^*E_{1y}+W^*E_{1z}\right]\times\frac{1}{k_{||}v_{||}+n\Omega_s+p\Omega_s+k_\perp\Delta'-\omega}\ , \tag{7}$$

where:

$$U^*=Cv_\perp\frac{n}{\lambda_1}-Cv_\perp\frac{n}{\lambda_1}\frac{\overline{E}'(x)}{4\Omega_s^2}+k_\perp v_\perp\xi''\frac{n}{\lambda_1}+k_\perp v_\perp\xi''\frac{\overline{E}'(x)}{4\Omega_s^2}\frac{n}{\lambda_1}\ ,$$

$$V^* = iCv_\perp \frac{J'_n(\lambda_1)}{J_n(\lambda_1)} + \frac{3}{4} Cv_\perp \frac{\overline{E'}(x) n}{\Omega_s^2 \lambda_1} - \Delta' C \ ,$$

$$W^* = \omega \frac{\partial f_{s0}}{\partial v_{||}} + Dk_\perp v_\perp \frac{n}{\lambda_1} + \frac{3Dk_\perp v_\perp}{4} \frac{\overline{E'}(x)}{\Omega_s^2} \frac{n}{\lambda_1} \ ,$$

$$C = (\omega - k_{||} v_{||}) \left(\frac{-2f_{s0}}{\alpha_{\perp s}^2} \right) + k_{||} \frac{\partial f_{s0}}{\partial v_{||}} \ ,$$

$$D = v_{||} \left(\frac{2f_{s0}}{\alpha_{\perp s}^2} \right) - \frac{\partial f_{s0}}{\partial v_{||}} \ ,$$

$$\lambda_1 = \frac{k_\perp v_\perp}{\Omega_s} \ , \ \lambda_2 = \frac{3}{4} \frac{k_\perp v_\perp \overline{E'}(x)}{\Omega_s^3} \ , \ J_n'(\lambda_1) = \frac{J_n(\lambda_1)}{d\lambda_1} \ .$$

Here, $\mathrm{J_n}(\lambda_1)$ is the Bessel's function and the well-known Bessel identity $e^{i\lambda_1 \sin\theta} = \sum_{n=-\infty}^{\infty} J_n(\lambda_1)\, e^{in\theta}$ is used.

The unperturbed bi-Maxwellian distribution function is written as:

$$f_{s0} = f_{sm0} + v_{0y}\xi'' \ , \tag{8}$$

$$\xi'' = \frac{1}{\Omega_s} \left[\frac{2(v_{||} - v_{0z}(x))}{\alpha_{||s}^2} \frac{\delta v_{0z}(x)}{\delta x} \right] f_{smo} \ ,$$

$$f_{mo} = \frac{n_0(x)}{(\pi)^{1/2} \alpha_{\perp s}^2 \alpha_{||s}} \exp\left[-\frac{(v_{0x}^2 - v_{0y}^2)}{\alpha_{\perp s}^2} - \frac{(v_{||} - v_{0z}(x))^2}{\alpha_{||s}^2} \right].$$

Here, ξ” is being the constant of motion and $n_0(x)$ is the plasma particle density.

$$\alpha_{\perp s} = \left(\frac{2k_B T_{\perp s}}{m_s} \right)^{1/2} \ , \quad \alpha_{||s} = \left(\frac{2k_B T_{||s}}{m_s} \right)^{1/2} \ .$$

Now simplifying *m* = *n*, *g* = *p* and using the definitions of current density, conductivity and dielectric tensor, we get the dielectric tensor:

$$\|\varepsilon(k_1 \omega)\| = 1 - \frac{4\pi \ e_s^2}{m_s \omega^2} \int \frac{d^3 v \sum J_p^2(\lambda_2) ||S_{ij}||}{k_{||} v_{||} + n\Omega_s + p\Omega_s + k_\perp \Delta' - \ \omega} \ , \tag{9}$$

where:

$$\|S_{ij}\| = \begin{vmatrix} J_n^2 U^* \frac{n}{\lambda_1} v_\perp & J_n^2 V^* \frac{n}{\lambda_1} v_\perp & J_n^2 W^* \frac{n}{\lambda_1} v_\perp \\ -iJ_n J_n' U^* v_\perp & -iJ_n J_n' V^* v_\perp & -iJ_n J_n' W^* v_\perp \\ J_n^2 U^* v_{||} & J_n^2 V^* v_{||} & J_n^2 W^* v_{||} \end{vmatrix} .$$

Now we consider the electrostatic ion-cyclotron instability.

$$\| \varepsilon_{||} \| = \mathrm{N}^2 . \tag{10}$$

Here, N is the refractive index.

The required electrostatic dispersion relation can be obtained by using the approximation of Huba [33] and from equations (8)–(10).

$$\mathrm{D}(\mathrm{k}, \omega) = 1 + \frac{2\omega_{\mathrm{ps}}^2}{\mathrm{k}_\perp^2 \alpha_{\perp \mathrm{s}}^2} \Gamma_{\mathrm{n}}(\mu_{\mathrm{s}}) \sum \mathrm{J}_{\mathrm{P}}^2(\lambda_2) \left[1 - \frac{\mathrm{E}'(\mathrm{x})}{4\Omega_s^2} \right] \frac{\mathrm{k}_\perp}{\mathrm{k}_{||}} \times$$

$$\times\left[\left(\frac{\bar{\omega}}{k_{\|}\alpha_{\|s}}-\frac{1}{2}\varepsilon_n\rho_s\frac{\alpha_{\perp s}}{\alpha_{\|s}}\right)Z(\xi)-A_s\frac{\alpha_{\perp s}^2}{\alpha_{\|s}^2}\left(1+\xi Z(\xi)\right)+A_T\frac{k_{\|}}{k_{\perp}}\left(1+\xi Z(\xi)\right)\right], \tag{11}$$

where:

$$\xi=\frac{\bar{\omega}-(n+p)\Omega_s-k_{\perp}\Delta'}{k_{\|}\alpha_{\|s}},$$

$$A_s=\frac{1}{\Omega_s}\frac{\delta v_{oz}(x)}{\delta x},\quad \varepsilon_n=\frac{\delta\ \ln\ n_0(x)}{\delta x},\quad A_T=\frac{\alpha_{\perp s}^2}{\alpha_{\|s}^2}-1,\quad \bar{\omega}=\omega-k_{\|}v_{oz}(x),\quad \lambda_{Ds}^2=\frac{\alpha_{\perp s}^2}{2\omega_{ps}^2},$$

$$\Gamma_n(\mu_s)=\exp(-\mu_s)I_n(\mu_s),\quad \mu_s=\frac{k_{\perp}^2\rho_i^2}{2}.$$

Here, $Z(\xi)$ is the plasma dispersion function [34], ω_{ps}^2 is the plasma frequency and $I_n(\mu_s)$ is the modified Bessel's function of order n.

Above dispersion relation reduces to that of Huba [33] if inhomogeneous DC electric field is removed and further using $\alpha_{\perp s}=\alpha_{\|s}$ and following of the assumptions of Pandey et al. [35], in order to get the dispersion relation for electrons and ions (s = i, e) the approximation for electrons are assumed as $k_{\perp}\rho_e<<1$ and for ions no such assumption is done. Thus, above equation becomes:

$$D(k,\omega)=1+\frac{1}{k_{\perp}^2\lambda_{De}^2}\eta_e\frac{T_{\perp e}}{T_{\|e}}+\frac{1}{k_{\perp}^2\lambda_{Di}^2}\eta_i\left[\frac{T_{\perp i}}{T_{\|i}}\Gamma_n(\mu_i)\frac{k_{\perp}}{k_{\|}}\left[\left(\frac{\bar{\omega}}{k\alpha_{\|i}}\times\frac{T_{\perp i}}{T_{\|i}}-\frac{1}{2}\varepsilon_n\rho_s\frac{\alpha_{\perp i}}{\alpha_{\|i}}+\right.\right.\right.$$

$$\left.\left.\left.+\frac{n\Omega_i+k_{\perp}\Delta'}{k_{\|}\alpha_{\|i}}\left(1-\frac{T_{\perp i}}{T_{\|i}}\right)\right)Z(\xi_i)-A_i\frac{T_{\perp i}}{T_{\|i}}\left(1+\xi Z(\xi_i)\right)\right]\right]. \tag{12}$$

Substitution of the asymptotic expansion of $Z(\xi_i)=-\frac{1}{\xi_i}-\frac{1}{2\xi_i^3}$ for ions i.e. $|\xi_i|<<1$ [34] and $n_{0i}=n_{0e}$ with further multiplying throughout by $\frac{k_{\perp}^2\lambda_{Di}^2}{\eta_i}$ leads to:

$$0=\frac{\lambda_{Di}^2}{\lambda_{De}^2}\frac{\eta_e}{\eta_i}\frac{T_{\perp e}}{T_{\|e}}+\frac{T_{\perp i}}{T_{\|i}}-\Gamma_n(\mu_i)\frac{T_{\perp i}}{T_{\|i}}+\frac{\Gamma_n(\mu_i)k_{\perp}}{2k_{\|}}\varepsilon_n\rho_i\frac{\alpha_{\perp s}}{\alpha_{\|s}}\frac{k_{\|}\alpha_{\|i}}{\bar{\omega}-n\Omega_i-k_{\perp}\Delta'}-$$

$$-\frac{\Gamma_n(\mu_i)k_{\perp}}{k_{\|}}\frac{n\Omega_i+k_{\|}\alpha_{\|i}}{\bar{\omega}-n\Omega_i-k_{\perp}\Delta'}-\frac{\Gamma_n(\mu_i)k_{\perp}}{2\left(\bar{\omega}-n\Omega_i-k_{\perp}\Delta'\right)^2}.\frac{T_{\perp i}}{T_{\|i}}\left(k_{\|}\alpha_{\|i}\right)^2\left(1-\frac{k_{\perp}}{k_{\|}}A_i\right), \tag{13}$$

where:

$$\eta_i=1-\frac{\overline{E_i'}(x)}{4\Omega_i^2},\quad \eta_e=1-\frac{\overline{E'_e}(x)}{4\Omega_e^2}.$$

Multiplying equation (13) throughout by $\left(\frac{\bar{\omega}-n\Omega_i-k_{\perp}\Delta'}{k_{\|}\alpha_{\|i}}\right)^2$, we obtain a quadratic equation as:

$$a_1\left(\frac{\bar{\omega}'}{\Omega_i}\right)^2+b_1\left(\frac{\bar{\omega}'}{\Omega_i}\right)+c_1=0, \tag{14}$$

where:

$$a_1=a_2\left(\frac{\Omega_i}{k_{\|}\alpha_{\|}}\right)^2,\quad a_2=\frac{\eta_e}{\eta_i}\frac{T_{\perp i}}{T_{\|i}}+\frac{T_{\perp i}}{T_{\|i}}-\Gamma_n(\mu_i)\frac{T_{\perp i}}{T_{\|i}},$$

$$b_1 = \frac{\Omega_i}{k_{||}\alpha_{||i}} b_2 - \frac{2k_\perp \Delta'}{k_{||}^2 \alpha_{||i}^2} a_2 \Omega_i\ ,\ b_2 = \frac{\Gamma_n(\mu_i) k_\perp}{2k_{||}} \varepsilon_n \rho_i \frac{\alpha_{\perp i}}{\alpha_{||i}} - \frac{\Gamma_n(\mu_i) k_\perp}{2k_{||}} - \frac{\Gamma_n(\mu_i) k_\perp n \Omega_i}{2k_{||}^2 \alpha_{||i}}\ ,$$

$$c_1 = \frac{\Gamma_n(\mu_i) T_{\perp i}}{2T_{||i}} \left(1 - \frac{k_\perp}{k_{||}} A_i\right) - \frac{b_2 k_\perp \Delta'}{k_{||}\alpha_{||i}} + \frac{k_\perp^2 \Delta'^2}{k_{||}^2 \alpha_{||i}^2}\ ,$$

$$\overline{\omega}' = \overline{\omega} - n\Omega_i\ .$$

The solution of equation (14) is:

$$\frac{\overline{\omega'}}{\Omega_i} = -\frac{b_1}{2a_1}\left[1 \pm \sqrt{\left(1 - \frac{4a_1 c_1}{b_1^2}\right)}\ \right]. \tag{15}$$

From this expression the dimensionless growth rate has been calculated by computer technique when $b_1^2 < 4a_1 c_1$ and also the dimensionless real frequency has been calculated from above expression. Hence, this criterion gives a condition for the growth rate of wave with homogeneous DC electric field considering inhomogeneity in electric field is neglected. It means we have discussed the case of homogeneous DC electric field.

Result and Discussion

In this section, we show the solution of the equation (15) for x^2/a^2 <1 using parameters like a magnetic field, density gradient , thermal velocities and etc. which were representative of laboratory by Kim and Merlino [16] and Rosenberg, Merlino [17]. We consider plasma in which the heavy positive ions are produced due to ionization of K^+ and light electron are produced from SF_6^-. It is assumed that electron and ion temperature ratio $\frac{T_e}{T_i}$ is varying between 2 to 4. It is further assumed that the plasma is immersed in a magnetic field whose strengths are varying from 0.24 to 0.32 T and homogeneous DC electric field strength from 4 V/m to 12 V/m which is perpendicular to magnetic field. In this case the positive ions gyro-radius ρ~ 0.095 cm having a temperature anisotropy $A_T = \frac{T_{\perp i}}{T_{\|i}} - 1$ varying from 0.5 to 1.5 with density gradient $\varepsilon_n \rho_i$ =0.2 has been considered. In this case we would expect that the electrostatic ion cyclotron instability could become excited by parallel velocity shear with scale length A_i varying from 0.5 to 0.55.

In fig. 1 the variation of growth rate $\frac{\gamma}{\Omega_i}$ versus $k_\perp \rho_i$ for different values of velocity shear scale length A_i has been shown for other fixed plasma parameters. The growth rate increases with increasing value of shear scale length A_i and the bandwidth slightly increases with A_i but the maxima of band does not shift. The maximum peak value of growth rate is 4.05×10^{-3} at $k_\perp \rho_i$ =2, A_i=0.55. The mechanism for instability of this mode is due to coupling of regions of positive and negative wave energy. This coupling occurs if velocity shear is non-uniform and hence velocity shear is the source of instability.

Fig. 2 shows the variation of growth rate $\frac{\gamma}{\Omega_i}$ versus $k_\perp \rho_i$ for various values of electron ion temperature ratio $\frac{T_e}{T_i}$, on this figure the growth rate increases by increasing the values of electron ion temperature ratio because due to inhomogeneity in electron ion temperature that depends on the applied voltage of electrodes. The maximum peak values of growth rate is 3.85×10^{-3} at the $k_\perp \rho_i$ =2 with homogeneous DC electric field, as velocity shear term is proportional to electron ion temperature ratio $\frac{T_e}{T_i}$.

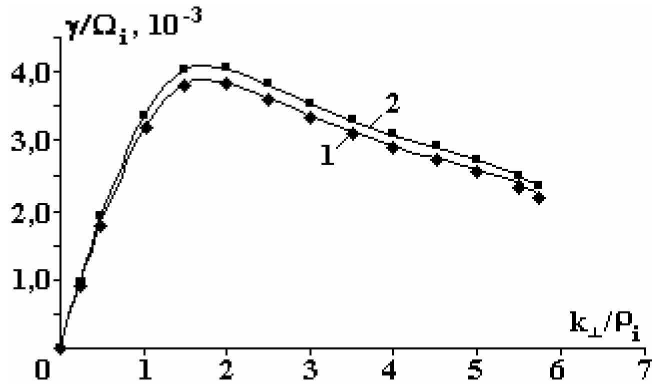

Fig. 1. Variation of growth rate γ/Ω_i *versus* $k_\perp\rho_i$ *for different values of* A_i *and other parameters are* B_0*=0.24 T,* T_e/T_i*=2,* E_0*=8 V/m,* θ *= 88.5*^{0}*,* A_T *=1.5,* $\varepsilon_n\rho_i$*=0.2. 1 –* A_i *= 0,5; 2 –* A_i *= 0,55*

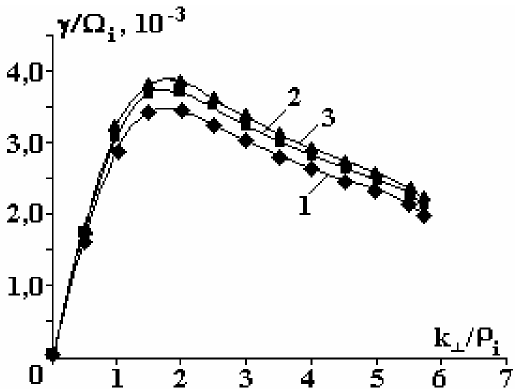

Fig. 2. Variation of growth rate γ/Ω_i *versus* $k_\perp\rho_i$ *for different values of* T_e/T_i *and other parameters are* A_i *=0.5,* B_0*=0.24 T,* E_0*=8 V/m,* θ *= 88.5*^{0}*,* A_T*=1.5,* $\varepsilon_n\rho_i$*=0.2. 1 –* T_e/T_i *= 2; 2 –* T_e/T_i *= 3; 3 –* T_e/T_i *= 4*

Fig. 3,*a* and *b* show the variation of real frequency $\frac{\omega_r}{\Omega_i}$ (ω_r is a real frequency) and growth rate $\frac{\gamma}{\Omega_i}$ versus $k_\perp\rho_i$ for different values of magnetic field strength B_0 with other fixed parameters listed in figure caption. The growth rate and real frequency decrease with increasing the magnetic field strength. Due to change in magnetic field gyro-frequency has been changed. The homogeneous magnetic field couples positive and negative energy waves thus changes the growth rate of the wave. The magnetic field strength is a useful parameter for required velocity of EIC wave. Hence, this is useful result for designing a machine for cold spray & metal cutting operations.

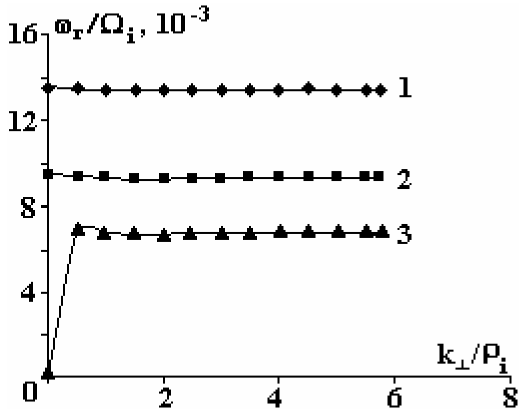

Fig. 3,a. Variation of real frequency ω_r/Ω_i *versus* $k_\perp\rho_i$ *for different values of* B_0 *and other parameters are* A_i *=0.5,* T_e/T_i*=2,* E_0*=8 V/m,* θ_1 *= 88.5*^{0}*,* A_T*=1.5,* $\varepsilon_n\rho_i$*=0.2. 1 –* B_0 *= 0,2 T; 2 –* B_0 *= 0,24 T; 3 –* B_0 *= 0,28 T*

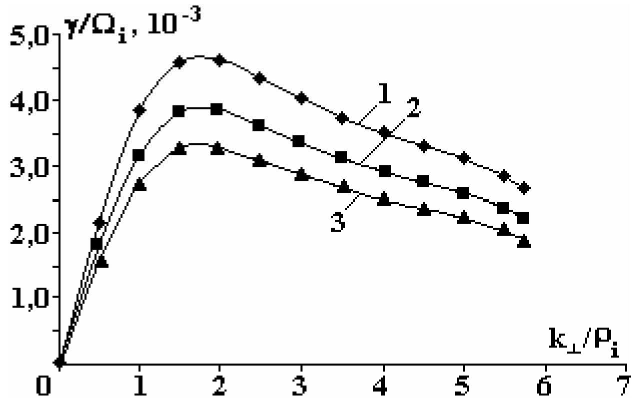

Fig. 3,b. Variation of growth rate γ/Ω_i *versus* $k_\perp\rho_i$ *for different values of* B_0 *and other parameters are* A_i *=0.5,* T_e/T_i*=2,* E_0*=8 V/m,* θ *= 88.5*^{0}*,* A_T*=1.5,* $\varepsilon_n\rho_i$*=0.2. 1 –* B_0 *= 0,2 T; 2 –* B_0 *= 0,24 T; 3 –* B_0 *= 0,28 T*

Fig. 4,*a* and *b* shows the variation of real frequency $\frac{\omega_r}{\Omega_i}$ and growth rate $\frac{\gamma}{\Omega_i}$ versus $k_\perp\rho_i$ for various values of homogeneous DC electric field. The growth rate deceases with increasing of the value of homogeneous DC electric field from 4 V/m to 12 V/m. But the real frequency increases with increasing the value of electric field. In general, this has a stabilizing effect introducing to the resonant and non-resonant interactions affecting on the growth rate and real frequency. This result will be helpful for designing the machine like a cold spray and metal cutting to control the frequency and velocity of the wave. The velocity of EIC wave is 1011 m/s for the value of homogeneous DC electric field 8 V/m and it is 2527 m/s for 20 V/m with other fixed parameters listed in figure caption.

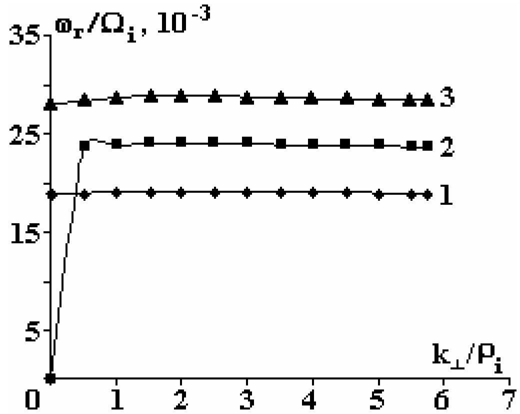

Fig. 4,a.Variation of real frequency ω_r/Ω_i *versus* $k_\perp\rho_i$ *for different values of* E_0 *and other parameters are* A_i *=0.5,* B_0*=0.24 T,* T_e/T_i*=2,* θ *= 88.5*^{0}*,* A_T*=1.5,* $\varepsilon_n\rho_i$*=0.2. 1 –* E_0 *= 16 V/m; 2 –* E_0 *= 20 V/m; 3 –* E_0 *= 24 V/m*

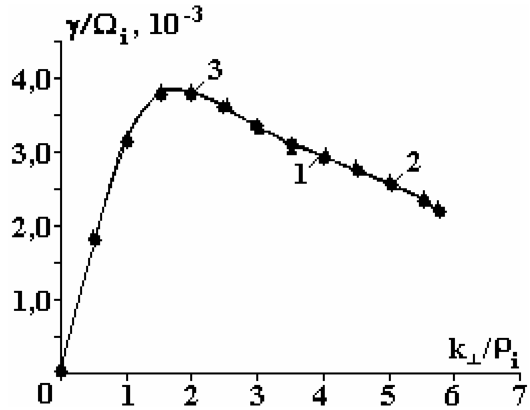

Fig. 4,b. Variation of growth rate γ/Ω_i *versus* $k_\perp\rho_i$ *for different values of* E_0 *and other parameters are* A_i *=0.5,* B_0*=0.24 T,* T_e/T_i*=2,* θ *= 88.5*^{0}*,* A_T*=1.5,* $\varepsilon_n\rho_i$*=0.2. 1 –* E_0 *= 16 V/m; 2 –* E_0 *= 20 V/m; 3 –* E_0 *= 24 V/m*

Fig. 5 shows the variation of growth rate versus angle between wave number $k_\perp$ and $k_\parallel$ like θ with parameter listed in figure caption. The maximum growth rate obtained for θ=88.5^0. The parameters like a density gradient $\varepsilon_n\rho_i$ and temperature anisotropy $A_T = \frac{T_{\perp i}}{T_{\parallel i}} - 1$ have less effect on growth rate but the growth rate increases slightly with increasing the values of $\varepsilon_n\rho_i$ and A_T .

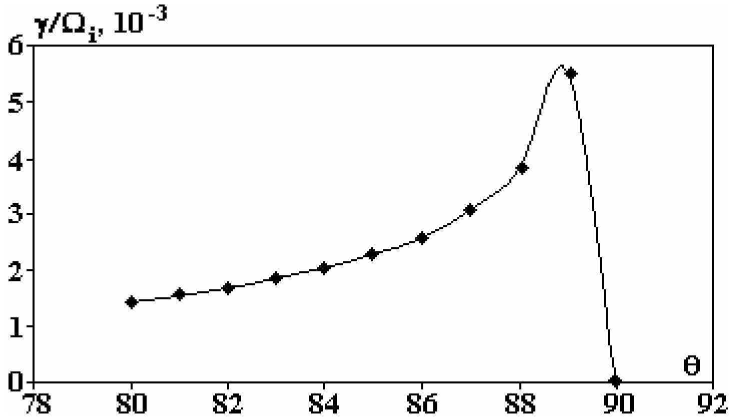

Fig. 5. Variation of growth rate γ/Ω_i *versus* θ *for parameters like* $k_\perp\rho_i$ *=2,* A_i*=0.5,* B_0*=0.24 T,* T_e/T_i*=2,* E_0*=8 V/m,* A_T*=1.5,* $\varepsilon_n\rho_i$*=0.2*

Conclusion

In this paper the effect of magnetic field, electric field, electron ion temperature ratio, temperature anisotropy of ions, shear scale length and density gradient on the growth rate and real frequency have been discussed separately. This result is useful for designing machine for cold spray & metal cutting operations with help of required velocity of generated and excited EIC wave.

Acknowledgement: I thank the reviewer for very useful suggestions which have been incorporated at appropriate places.

REFERENCES

1. Ganguli G., Lee Y.C., and Palmadesso P. Electrostatic ion-cyclotron instability caused by a nonuniform electric field perpendicular to the external magnetic field. *Phys. Fluids*. 1985, **28**(3), 761–763.

2. Ganguli G., Lee Y.C., and Palmadesso P.J. Kinetic theory of electrostatic waves due to transverse velocity shears. *Phys. Fluids*. 1988, **31**(4), 823–838.
3. Nishikawa K.-I., Ganguli G., Lee Y.C., and Palmadesso P.J. Simulation of ion-cyclotron-like modes in a magnetoplasma with transverse inhomogeneous electric field. *Phys. Fluids*. 1988, **31**(6), 1568–1576.
4. Waelbroeck F.L. and Chen L. Ballooning instabilities in tokamaks with sheared toroidal flows. *Phys. Fluids B*. 1991, **3**(3), 601–610.
5. Maslowe S.A. *Shear flow instabilities and transition, in: Hydrodynamic Instabilities and the Transition to Turbulence.* (H.L. Swinney and J.P. Gollub, Eds.). Berlin: Spinger-Verlag, 1985. Ch.7, pp.181–228.
6. Bhattacharjee A., Iacono R., Milovich J.L., and Paranicas C. Ballooning stability of axisymmetric plasmas with sheared equilibrium flows. *Phys. Fluids B*. 1989, **1**(11)**,** 2207–2212.
7. Biglari H., Diamond P.H., and Terry P.W. Influence of sheared poloidal rotation on edge turbulence. *Phys. Fluids B*. 1990, **2**(1), 1–4.
8. Shaing K.C. and Crume (Jr.) E.C., Bifurcation theory of poloidal rotation in tokamaks: A model for *L-H* transition. *Phys. Rev. Lett*. 1989, **63**(21), 2369–2372.
9. Groebner R.J., Burrell K.H., and Seraydarian R.P. Role of edge electric field and poloidal rotation in the *L-H* transition. *Phys. Rev. Lett*. 1990, **64**(25), 3015–3018.
10. Ganguli G., Slinker S., Gavrishchaka V. and Scales W. Low frequency oscillations in a plasma with spatially variable field-aligned flow. *Phys. Plasmas*. 2002, **9**(5), 2321–2329.
11. Merlino R.L., Agrimson E.P. Kim S.-H., D'Angelo N., Ganguli G.I. Laboratory studies of the effect of parallel velocity shear on electrostatic ion waves in magnetized plasma. *Proceeding of XXIX General Assembly of Union Radio Scientifique Internationale.* Chicago, USA, 7-16th August 2008, H05.1, p.170 (4 pages).
12. D'Angelo N. Kelvin-Helmholtz instability in a fully ionized plasma in a magnetic field. *Phys. Fluids*. 1965, **8**(9), 1748–1750.
13. Merlino R.L. Electrostatic ion-cyclotron waves driven by parallel velocity shear. *Phys. Plasmas*. 2002, **9**(5), 1824–1825.
14. D'Angelo N. and Motley R.W. Electrostatic oscillations near the ion-cyclotron frequency. *Phys. Fluids*. 1962, **5**(5), 633–634.
15. Drummond W.E. and Rosenbluth M.N. Anomalous diffusion arising from microinstabilities in a plasma. *Phys. Fluids*. 1962, **5**(12), 1507–1513.
16. Kim S.-H. and Merlino R.L. Electron attachment to C_7F_{14} and SF_6 in a thermally ionized potassium plasma. *Phys. Rev. E*. 2007, **76**(3), 035401(R) [4 pages].
17. Rosenberg M. and Merlino R.L. Instability of higher harmonic electrostatic ion cyclotron waves in a negative ion plasma. *Journal of Plasma Physics*. 2009, **75**(04), 495–508.
18. Agrimson E.P., D'Angelo N. and Merlino R.L. Effect of parallel velocity shear on the excitation of electrostatic ion cyclotron waves. *Phys. Lett. A*. 2002, **293**(5–6), 260–265.
19. Teodorescu C., Reynolds E.W. and Koepke M.E. Observation of inverse ion-cyclotron damping induced by parallel velocity shear. *Phys. Rev. Lett*. 2002, **89**(10), 105001 [4 pages].
20. Agrimson E., Kim S.-H., D'Angelo N. and Merlino R.L. Effect of parallel velocity shear on the electron static ion-cyclotron instability in filamentary current. *Phys. Plasmas*. 2003, **10**(10), 3850–3852.
21. Akerstedt H.O. Velocity shear instabilition associated with plasma motion across a magnetic field. *Physica Scripta*. 1984, **29**(1), 75–86.
22. Akerstedt, H.O. The motion of a finite plasma slab across a transverse magnetic field. *Physica Scripta*. 1981, **24**(4), 775–784.
23. Noël, J.-M.A. *Small-scale electrodynamics in the auroral ionosphere.* The University of Western Ontario, 1999, Ph.D. dissertation.
24. Noël J.-M.A., St.-Maurice J.-P. and Blelly P.-L. Nonlinear model of short-scale electrodynamics in the auroral ionosphere. *Ann. Geophys*. 2000, **18**(9), 1128–1144.
25. Noël J.-M.A., St.-Maurice J.-P. and Blelly P.-L. The effect of *E*-region wave heating on electrodynamical structures. *Ann. Geophys*. 2005, **23**(6), 2081–2094.
26. Rother M., Schlegel K. and Lühr H. CHAMP observation of intense kilometer-scale field-aligned currents, evidence for an ionospheric Alfvén resonator. *Ann. Geophys*. 2007, **25**(7), 1603–1615.
27. Gavrishchaka V.V., Ganguli S.B. and Ganguli G.I. Origin of low-frequency oscillations in the ionosphere. *Phys. Rev. Lett*. 1998, **80**(4), 728–731.
28. Gavrishchaka V.V., Ganguli S.B., and Ganguli G.I. Electrostatic oscillations due to filamentary structures in the magnetic field-aligned flow: The ion-acoustic branch. *J. Geophys. Res*. 1999, **104**(A6), 12683–12693.

29. Basu B., and Coppi B. Velocity shear and fluctuations in the auroral regions of the ionosphere. *J. Geophys. Res.* 1989, **94**(A5), 5316–5326.
30. Misra K.D. and Pandey R.S. Generation of whistler emissions by injection of hot electrons in the presence of a perpendicular AC electric field. *J. Geophys. Res*. 1995, **100**(A10), 19405–19411.
31. Pandey R.S., Misra K.D., and Tripathi A.K. Kelvin-Helmholtz instability in an anisotropic magneto-plasma in the presence of inhomogeneous perpendicular electric field and parallel flow velocity shear. *Indian J. Radio Space Phys*. 2001, **30**, 113–120.
32. Misra K.D. and Tiwari M.S. Particle aspect analysis of $E\times B$ drift instability in the presence of non-uniform electric field. *Physica Scripta*. 1977, **16**(3-4), 142–146.
33. Huba J.D. The Kelvin-Helmholtz instability in inhomogeneous plasmas. *J. Geophys. Res*. 1981, **86**(A5), 3653–3656.
34. Fried B.D. and Conte S.D. *The Plasma Dispersion Function.* New York: Academic Press, 1961.
35. Pandey R.S., Misra K.D. and Tripathi A.K. Generation of ion-cyclotron wave by parallel flow velocity shear in the presence of inhomogeneous electric field in an anisotropic magneto-plasma. *Indian J. Radio Space Phys.* 2003, **32**, 75–82.

Received 02.09.10
Accepted 14.03.11

Summary

Analysis and study of parallel flow velocity shear and electrostatic ion cyclotron (EIC) instability have been done in plasma containing massive positive ions and electron by using the method of characteristics solution and kinetic theory in the presence of homogeneous direct-current (DC) electric field perpendicular to ambient magnetic field. The effect of many parameters on growth rate and real frequency has been discussed by using the experimental data. Applications to possible laboratory plasmas and industries are also discussed.